Plasma Potential and Turbulence Dynamics in Toroidal Devices (the Survey of T-10 and TJ-II Experiments)

A.V. Melnikov 1), L.G. Eliseev 1), C. Hidalgo 2), E. Ascasibar 2), A.A. Chmyga 3), R. Jiménez-Gómez 2), I.A. Krasilnikov 1), L.I. Krupnik 3), S.M. Khrebtov 3), A.D. Komarov 3), A.S. Kozachek 3), S.E. Lysenko 1), K. S. Dyabilin 1), V.A. Mavrin 1), J.L. de Pablos 2), I. Pastor 2), S.V. Perfilov 1), M.A. Pedrosa 2), R. Shurygin 1), A.I. Zhezhera 3), T-10 team 1) and TJ-II team 2)

1) Institute of Tokamak Physics, RRC "Kurchatov Institute", Moscow, Russia
2) Laboratorio Nacional de Fusión, EURATOM-CIEMAT, Madrid, Spain
3) Institute of Plasma Physics, NSC KhIPT, Kharkov, Ukraine

E-mail contact of main author: melnikov_07@yahoo.com

Abstract. The direct study of the electric potential and its fluctuations for comparable plasma conditions in the T-10 tokamak and TJ-II stellarator by HIBP diagnostics has been done. The following similar features of potential were founded: (i) the scale of several hundred Volts; (ii) the negative sign for densities $n_e > 1\times10^{19}$ m^{-3}, and comparable values in spite of the different heating methods; (iii) when n_e or τ_E rises, the potential evolves to negative direction; (iv) with ECR heating and associated T_e rise, τ_E degrades and the potential evolves to positive direction. Modeling shows that neoclassical mechanisms give significant contribution in the core electric potential formation. Oscillations of potential in the range of Geodesic Acoustic Modes in T-10 and Alfvén Eigenmodes in TJ-II were observed.

1. Introduction

The direct measurement of the mean electric potential and its oscillatory component in the core plasma are of primary importance for understanding the role of the radial electric field E_r in confinement improvement mechanisms. A Heavy Ion Beam Probe (HIBP) diagnostic was used in the T-10 circular tokamak and in TJ-II (four-period flexible heliac with spiral plasma axis, to study the plasma potential with high spatial (< 1 cm) and temporal (1 μs) resolution in comparable plasma parameters, but in different magnetic configurations. Main parameters of both machines are collected in Table 1.

TABLE 1. COMPARISON OF T-10 AND TJ-II MACHINES

Parameter	**TJ-II**	**T-10**
$\langle R \rangle$, m	1.5	1.5
$\langle a \rangle_{lim}$, m	0.22	0.3
B_t, T	1.0	1.5 - 2.5
$\bar{n}_e$, 10^{19} m^{-3}	0.3–6	1 - 4
P_{ECRH}, kW	≤ 600	≤ 1600
P_{NBI}, kW	≤900	-
E_{beam}, keV	125	300
HIBP ion species	Cs+	Tl+
observation area	-1 < ρ < 1	+0.2 < ρ < 1

TABLE 2. PARAMETERS OF STUDIED T-10 REGIMES

Regime	$\bar{n}_e$, 10^{19} m^{-3}	E_r, V/cm	Δr, cm	B_t, T	I_p, kA	τ_E, ms
1-*l*	1.3	55	6-30	1.55	140	20
1-*h*	2.4	65	6-30	1.55	140	36
2-OH	2.5	70	7-22	2.08	165	38
2-EC	2.1	55/47	7-22	2.08	165/212	13/12
3	4.1	90	16-27	2.4	210	50

2. T-10 experiments

Parameters of studied regimes are shown in Table 2. OH and ECRH deuterium and helium plasmas ($\bar{n}_e$=1.0-4.1×10^{19} m^{-3}) in T-10 are characterized by a negative potential up to φ(0.2)= -1600 V at the central area. The potential profile is monotonically increasing towards the plasma edge [1]. Figure 1 shows that the density rise due to gas puffing is accompanied by increasing of negative potential (regime 1-l and l-h in Table 2). Contrary, the rise of T_e due to increase of ohmic or additional ECR heating (fig. 2) leads to decrease of the absolute value of negative potential (fig. 3). Regime 3 with higher density and τ_E is characterized by stronger negative core E_r (fig. 4). Neoclassical (NC) modeling performed for various T-10 regimes shows that the ambipolar electric field E_r^{NC} is close to experimental values with a numerical factor, which is less than 3 [2]; E_r^{NC} for the high-density ohmic regime is also shown in fig. 4. So, the neoclassical mechanisms give substantial contribution to E_r formation and dynamics in the bulk plasmas.

It is important to note that no any strong irregularities in the potential profile near the EC power deposition radius r_{EC} =15 cm were observed, see fig. 2. Similar effects were observed in both machines in regimes with modulation of EC power (figs. 5 and 6).

Comparison of the HIBP and Correlation Reflectometer (CR) data [3] is shown in figure 7. HIBP data shows that plasma column rotates with $E\times B$ drift velocity not as a rigid body due to the $B_t(R)$ dependence. The typical values for angular velocity is $\Omega_{E\times B} \sim 1.5\times10^4$ rad/s for the OH, and $\Omega_{E\times B} \sim 1.25\times10^4$ rad/s for ECRH stages. Broadband drift-wave turbulence tends to rotate together with the $E\times B$ driven bulk plasma. ECRH induced plasma confinement degradation (see regimes 2 OH and EC in Table 2) leads to the retarding of drift rotation.

Direct numerical calculation of the turbulent dynamics in the edge plasma by the 5-fields {φ, n, p_e, p_i, $V_{||}$} nonlinear two-fluid MHD Braginskij model explains the E_r dynamics due to the influence of the Reynolds stress, in turn caused by potential phase relations [4]. Figure 8 presents the modeled potential and E_r profiles at the computational area limited by the plasma edge and SOL.

3. TJ-II experiments

The typical discharge scenario with ECR and NBI heating is shown in figure 9. Low-density ECRH hydrogen and helium plasmas ($\bar{n}_e$=0.3-1.1×10^{19} m^{-3}) in TJ-II are characterized by a positive potential up to φ(0)= +1200 V at the centre [5]. The minor area of the negative potential may appear at the edge depending on the plasma density. The density rise due to gas puff or NBI fueling is accompanied by the decrease of potential, which evolves to smaller absolute values, becoming fully negative, if $\bar{n}_e$ > 1×10^{19} m^{-3}. However, if the density

approaches $\bar{n}_e$=1.7-2.5×10^{19} m^{-3}, the growth of potential saturates at φ(0)= -600 V. Figure 10 shows the E_r evolution with density rise, measured at the gradient area ρ=0.7 from positive to negative values. Contrary, an increase in T_e due to increasing of ECRH power leads to an increase in plasma potential (fig. 11). The same effect is seen during ECRH power modulation (see figs 5 and 6).

Neoclassical modeling based on the approach, developed in [6] and used analytical expressions for symmetric and asymmetric component of particle fluxes [7, 8] explains the E_r values and dynamics in the bulk plasma. Electron root dominates for low-density ECRH plasmas while ion root dominates in high density NBI plasmas [2]. Figure 12 shows experimental and the modeled potential and E_r profiles for ECRH plasma with $\bar{n}_e = 0.6\times10^{19}$ m^{-3}. Modeled potential profile, corresponding to ion root at the periphery fits the experimental data for these conditions.

Confinement degradation due to the increase of the ECRH power leads to positive trend of central potential (fig. 13). The similar effect was observed in T-10.

The L-H transition spontaneously happening in NBI heated plasmas [9] is characterized by a potential drop ~ -100 V, formation of the edge layer with a strong negative E_r~ -100 V/cm, and a strong suppression of the density fluctuations and turbulent particle flux $\tilde{\Gamma}_{E\times B}$ in the edge and bulk plasmas [10]. Figure 14 shows the typical plasma density spectrogram in the shot with a sequence L-H and H-L transitions. One may see the strong suppression of the broadband turbulence in the H-mode, manifested by H_α decay and W_{dia} increase, and recovery after back H-L transitions, indicated by H_α increase and W_{dia} decrease.

In both machines regimes with improved confinement induced by edge biasing were characterized by the formation of a strong edge E_r and suppression of potential and density turbulence [11]. Thus there is a clear link between the value of the electric potential, formation of an edge layer with strong negative radial electric field, turbulence suppression and increase in plasma density and confinement.

4. Study of oscillations

Various types of the quasi-coherent potential oscillations were studied in both machines in view of the link with turbulence. Geodesic Acoustic Modes (GAMs), high-frequency counterpart of zonal flows, may be possible mechanism of the turbulence self-regulation. The theory proposes the unified dispersion relation for GAMs and Beta induced Alfvén Eigenmodes (BAE) [12]. In T-10, the mode, identified as GAM, presents a dominant peak in the power spectral density of potential. In some cases a higher frequency satellite appears. (fig. 15) [13]. Mode is more pronounced during ECRH, when the typical frequencies are seen in the band 22-27 kHz over the whole plasma cross-section. In all regimes the mode frequency is close to a constant over the investigated radial interval (fig. 16), showing inconsistency with theoretical predictions in the plasma core [12]. However, at the edge, ρ = 0.95, the frequency is consistent with theoretical prediction [4] that may be indicative this mode is an edge driven spatially global eigenmode. The frequency weakly depends on the magnetic field and plasma density. With the density rise, first the satellite and then the main peak consequently disappear. The amplitude of GAM induced potential perturbations in T-10 may be quite significant, up to δφ = 100 V; they exhibit a high correlation with density oscillations. GAM modulation of the high frequency turbulence was also reported [14].

The core potential, density and B_{pol} oscillations caused by Alfvén Eigenmodes (AE) were studied in NBI heated TJ-II plasma and shown in fig. 14 (see details in [15]). Oscillating potential due to AEs was found to have a range $\delta\varphi = 10$ V, AE induced poloidal electric field δE_{pol}~10 V/cm [16]. AE contribution to the bulk plasma turbulent particle flux was found to be variable depending on the phase relations between E_{pol} and n_e oscillations.

5. Conclusions

Despite the large differences in the topology of the confining magnetic field between two machines, the electric potential shows the following striking similarities:
1. Similar magnitudes for the potential φ and electric field E_r;
2. For $\bar{n}_e > 1\times10^{19}$ m^{-3}, plasma potential is negative with comparable absolute values despite the use of different heating methods: OH and ECRH in T-10, ECRH and/or NBI in TJ-II;
3. An increase in n_e and τ_E is accompanied by similar changes in φ and E_r: both become more negative. Application of ECRH, causing a rise in T_e and a reduction in τ_E, results in more positive values for φ and E_r;
4. Spontaneous and biased transitions to improved confinement regimes are associated with more negative values for E_r and turbulence suppression.
5. Within the achieved experimental accuracy, the broadband drift-wave turbulence tends to rotate with the plasma E×B rotation velocity in T-10 tokamak.
6. Quasicoherent modes, interacting with ambient turbulence, like GAMs in T-10 and HAEs in TJ-II, have pronounced component in electric potential.
7. These results indicate the importance of φ and E_r in determining turbulence, and thus energy confinement: negative values are associated with better confinement in TJ-II and T-10.

Russian team is supported by RFBR Grants 10-02-01385 and 08-02-01326.

References

[1] MELNIKOV, A.V., et al., Proc. 37-th EPS Conf. on Plasma Physics (Dublin, 2010) O-5.128
[2] DYABILIN, K.S., et al., "Electric potential in TJ-II stellarator: experiment and simulation", Preprint RRC "Kurchatov Institute" (2010), in press.
[3] VERSHKOV, V.A., et al., Nucl. Fusion **47** (2005) S203.
[4] SHURYGIN, R.V. and MAVRIN, A.A., Plasma Phys. Reports **35** (2010) 579.
[5] MELNIKOV, A.V., et al., Fusion Sci. and Techn. **51** (2007) 31.
[6] MAASSBERG, H., et al., Phys. Fluids B **5** (1993) 3627.
[7] KOVRIZHNYKH, L.M., Nucl. Fusion **24** (1984) 851.
[8] HASTINGS, D.E., HOULBERG, W.A. and SHAING K.C. Nucl. Fusion **25** (1985) 445.
[9] ESTRADA, T., et al., Plasma Phys. Control. Fusion **51** (2009) 124015
[10] MELNIKOV, A.V., et al., Proc. 36-th EPS Conf. on Plasma Physics (Sofia, 2009) P-4.186.
[11] MELNIKOV, A.V., et al., Fusion Sci. and Techn. **46** (2004) 299.
[12] SMOLYAKOV, A.I., NGUEN, C. and GARBET, X., Nucl. Fusion **50** (2010) 054002.
[13] MELNIKOV, A.V., et al., Proc. 37-th EPS Conf. on Plasma Physics (Dublin, 2010) P-1.065.
[14] MELNIKOV, A.V., et al., Plasma Phys. Control. Fusion **48** (2006) S87.
[15] ELISEEV, L.G., et al., this conference, Rep. EXW/P7-17.
[16] MELNIKOV, A.V., et al., Nucl. Fusion **50** (2010) 084023.

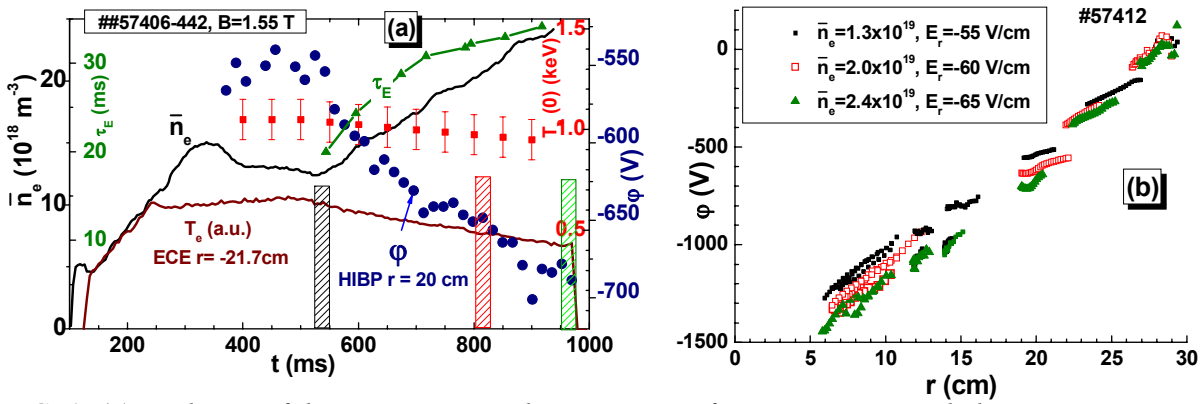

FIG. 1. (a) Evolution of density n_e, potential φ, energy confinement time τ_E and electron temperature $T_e(0)$ (■) in the low-B regime with density ramp-up. (b) The potential profile combined from the set of the scans for three densities in time instants marked by hatched rectangles in (a).

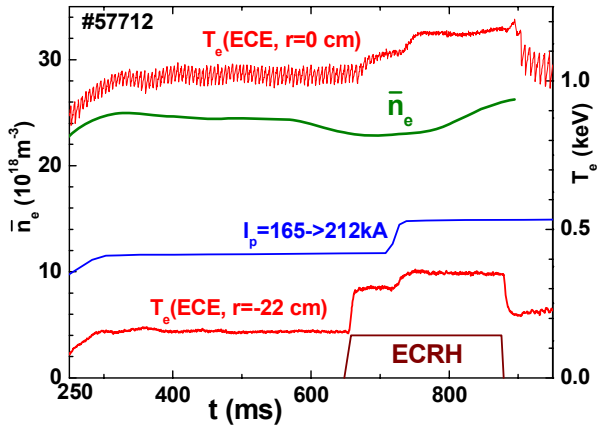

FIG. 2. Regime with additional ECR heating and current ramp-up.

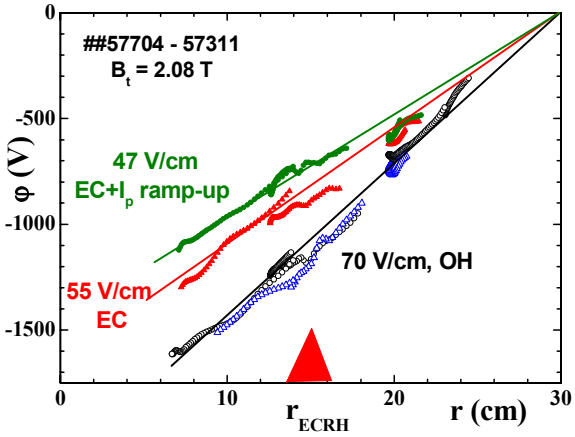

FIG. 3. The potential profile in regime with additional heating and current ramp-up; ▲ marks position of EC resonance.

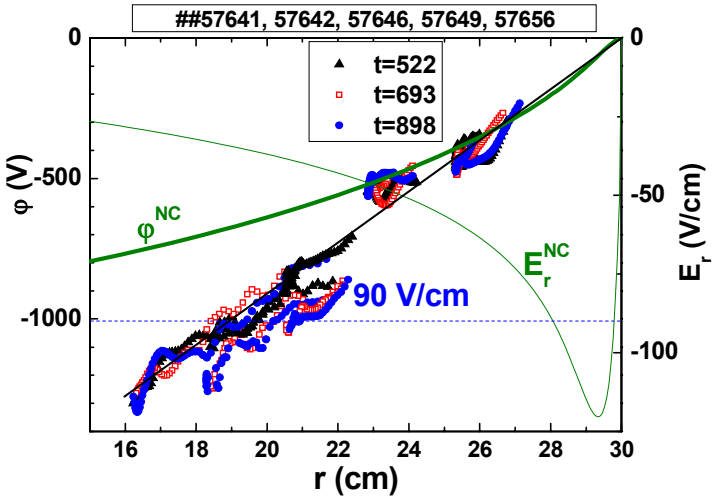

FIG. 4. The potential and electric field profiles in high-density ohmic regime. Symbols are experiment, green curves are neoclassical simulations.

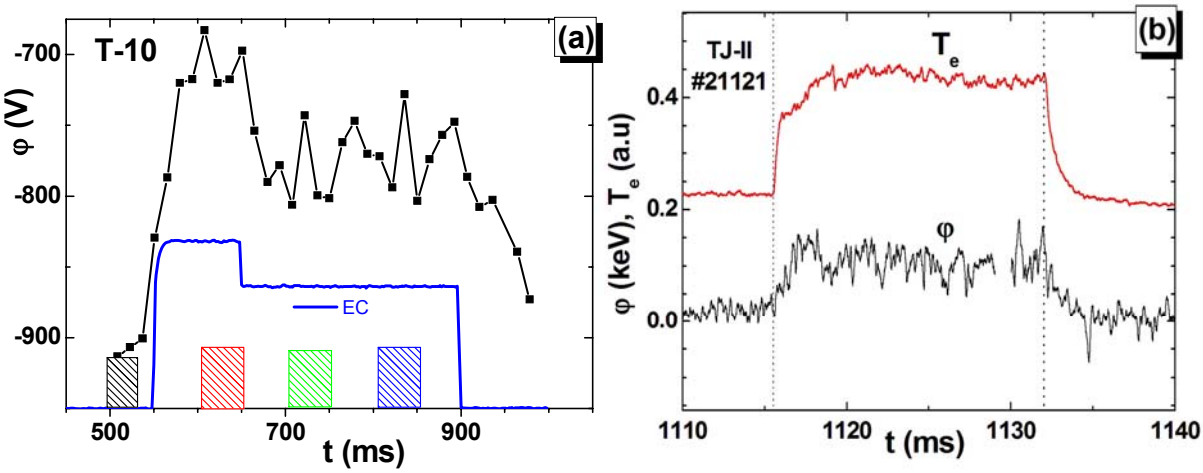

FIG. 5. Time evolution of potential in regimes with modulation of ECR heating in T-10 (a) and TJ-II (b).Hatched rectangles mark instants of potential measurements.

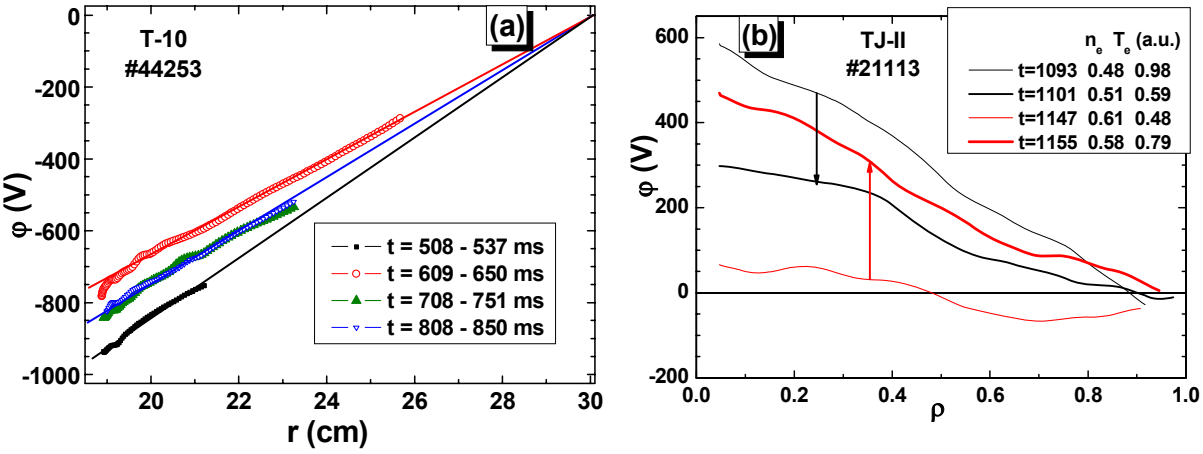

FIG. 6. Profiles of potential in regimes from figure 5 for T-10 (a) and TJ-II (b). Arrows show direction of evolution.

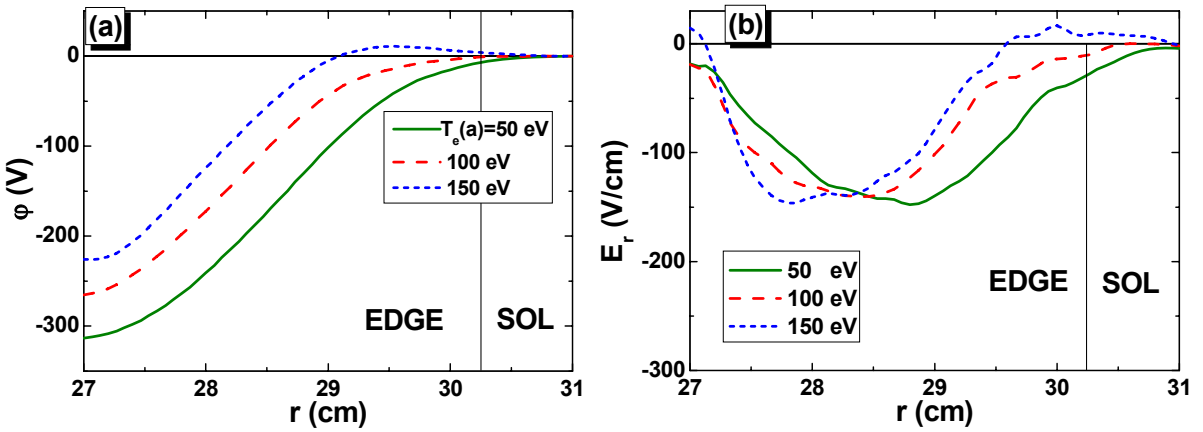

FIG. 7. Profiles of potential (a) and radial electric field (b) calculated with 5-fields two-fluid MHD model for different edge temperatures.

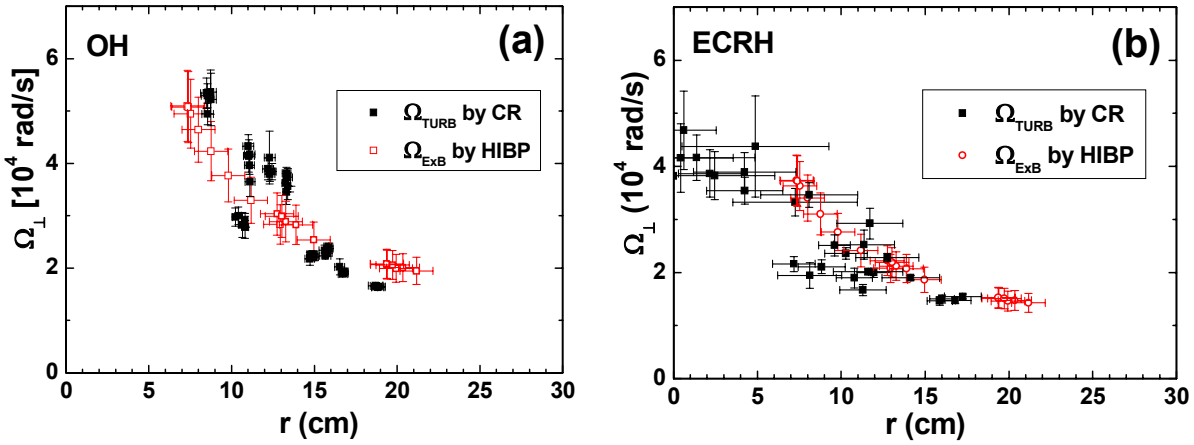

FIG. 8. Plasma E×B and turbulence rotation in regime 2, measured by correlation reflectometer (CR) and by heavy ion beam (HIBP) in ohmic (a) and ECR phases (b).

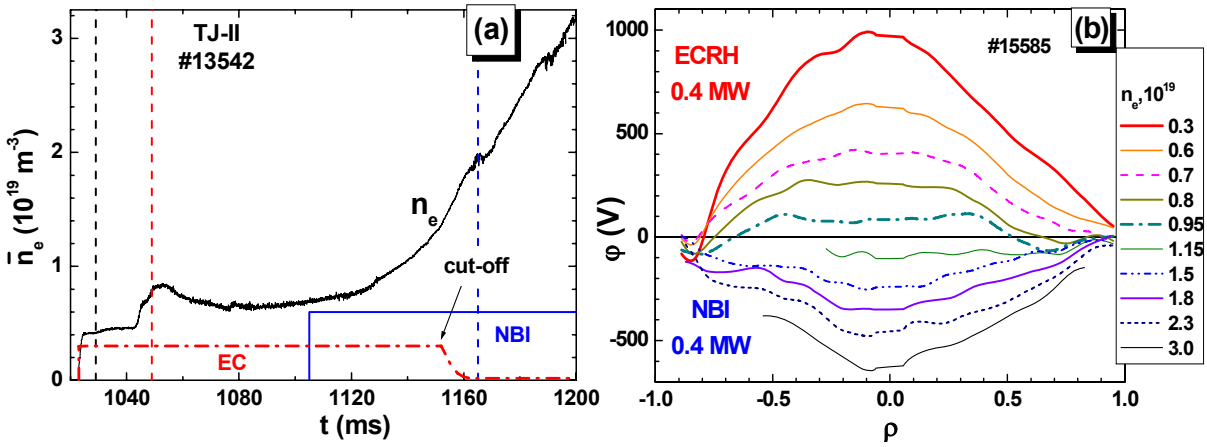

FIG. 9. Evolution of density (a) and potential (b) in regime with ECRH and NBI heating on TJ-II

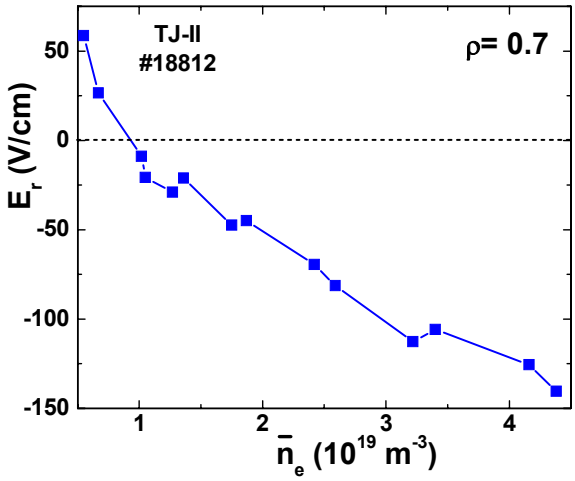

FIG. 10. Evolution of radial electric field in regime with density growth.

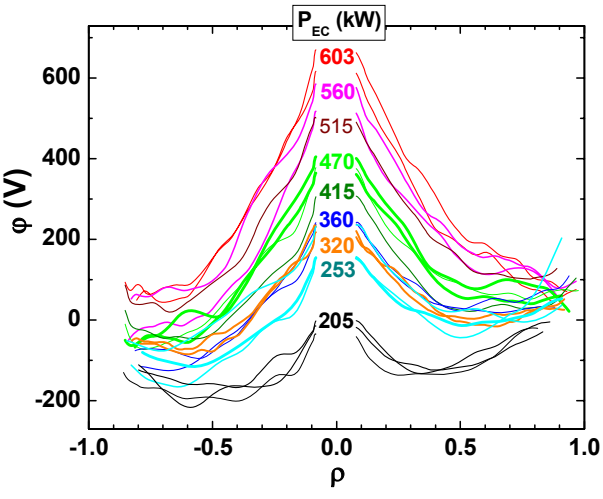

FIG. 11. Evolution of potential during EC power scan at fixed density $\bar{n}_e$=0.65×10^{19} m^{-3}.

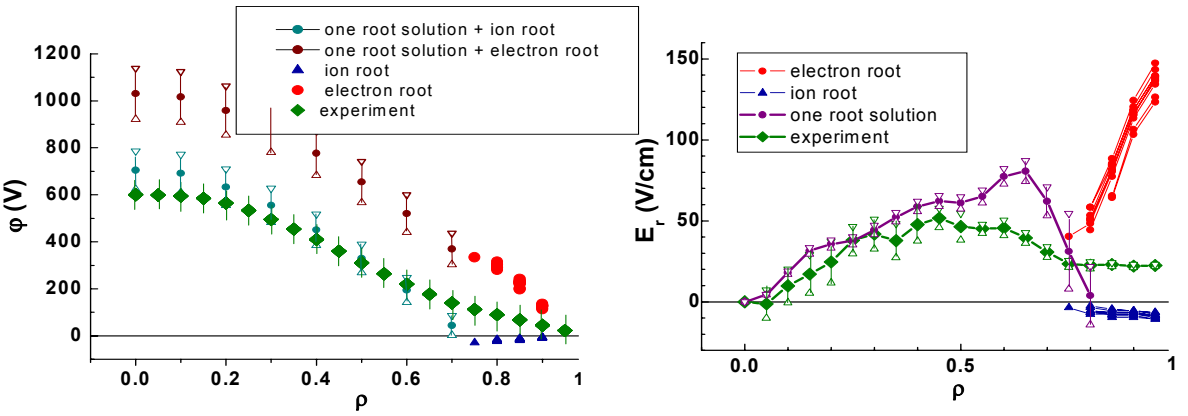

FIG. 12. Comparison of the neoclassical modeling with experiment for regime, presented in fig. 9 (low density n_e=0.6×10^{19} m^3, off-axis ECRH). Error bars for model curves denote 10% variation of plasma T_e, T_i and n_e profiles.

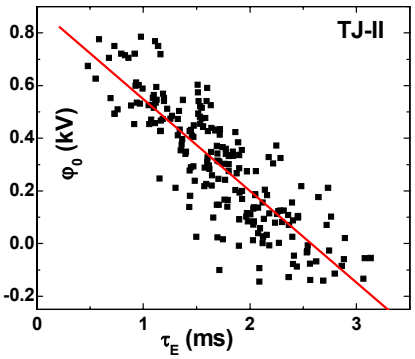

FIG. 13. Potential vs energy confinement time for shots shown in fig. 11.

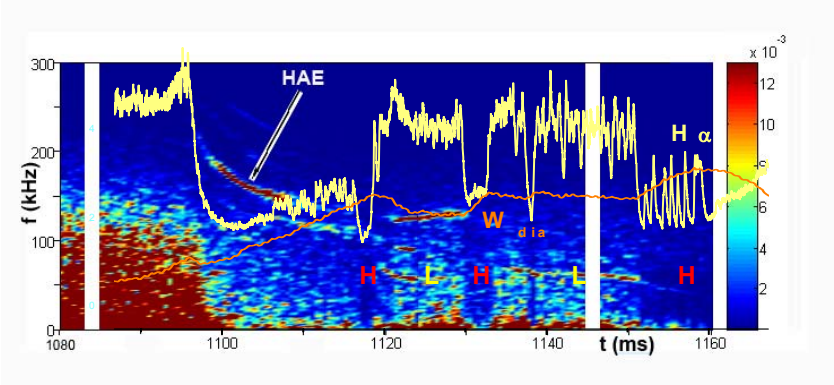

FIG. 14. Hα emission, energy content and spectrogram of plasma density oscillations in NBI regime with spontaneous L-H transitions. Quasi-coherent peaks present HAE.

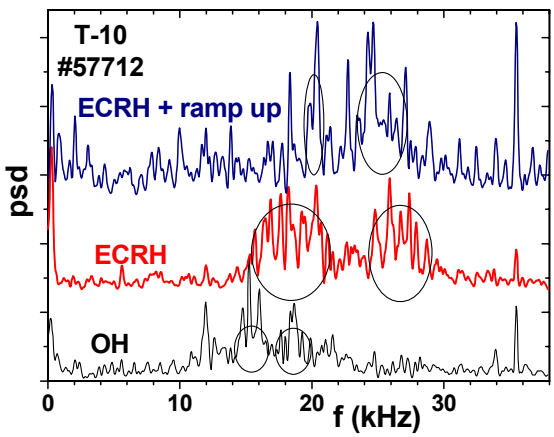

FIG. 15. Spectra of potential oscillations in regime 2. Peaks in ellipses are identified as GAMs and satellites.

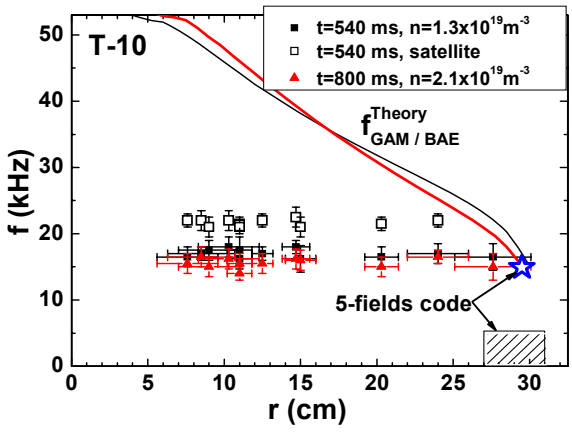

FIG. 16. Comparison of potential oscillations in regime 2 with analytical theory (lines) and 5-fields code calculations (star). Rectangle shows the region of the code validity.